Available online at www.sciencedirect.com
SCIENCE DIRECT
Journal of Controlled Release 111 (2006) 117–127
journal of controlled release
www.elsevier.com/locate/jconrel

Modeling the release of proteins from degrading crosslinked dextran microspheres using kinetic Monte Carlo simulations

Karin D.F. Vlugt-Wensink [a,c,*], Thijs J.H. Vlugt [b], Wim Jiskoot [a], Daan J.A. Crommelin [a,c], Ruud Verrijk [c], Wim E. Hennink [a]

[a] Department of Pharmaceutics, Utrecht Institute for Pharmaceutical Sciences (UIPS), Utrecht University, P.O. Box 80082, 3508 TB Utrecht, The Netherlands
[b] Condensed Matter and Interfaces, Debye Institute, Utrecht University, PO Box 80000, 3508 TA Utrecht, The Netherlands
[c] OctoPlus Technologies, OctoPlus b.v., Zernikedreef 12, 2333 CL, Leiden, The Netherlands

Received 30 September 2005; accepted 29 November 2005
Available online 23 January 2006

Abstract

To optimize and predict the release of proteins from biodegradable microspheres based on crosslinked dextran, a fundamental understanding of the mechanisms controlling their release is necessary. For that purpose, a mathematical model has been developed to describe the release of proteins from these hydrogel-based microspheres. A kinetic Monte Carlo scheme for the degradation of a small domain inside the microsphere was developed. The results from this were used in a second kinetic Monte Carlo scheme to model the diffusion and the subsequent release of proteins. The only processes included in this model are diffusion and degradation. The general effects of diffusion, crosslink density, protein loading, and clustering of proteins on the release were investigated. The model crosslink density (X_{model}) and the model diffusivity (D_{model}) were fitted to experimental release data of BSA monomer from hydroxyethyl methacrylated dextran (dex-HEMA) microspheres. By using the experimental release curves of liposomes and BSA monomer, it was found that (1) the model crosslink density (X_{model}) scales with the hydrodynamic diameter (d_{h}) as $d_{\mathrm{h}}^{1.64}$ and (2) the diffusivity of the protein (D_{model}) scales approximately with $1/d_{\mathrm{h}}$ (Stokes–Einstein). Using these scaling relations, quantitative predictions of the release curves of BSA dimer, immunoglobulin G and human growth hormone were possible. In conclusion, this model may play an important role in the optimization, understanding and prediction of the release of various proteins from degradable hydrogels.

Keywords: Biodegradation; Modeling; Protein release; Release mechanism; Monte Carlo simulation; Hydrogel

1. Introduction

Biodegradable hydrogels in the form of macroscopic (in situ forming) systems and injectable microparticles are attractive systems for the controlled release of pharmaceutically active proteins [1–6]. It has been shown that hydrogels have a good compatibility with proteins and living tissue [7–11]. Moreover, a unique property of hydrogels is the possibility to tailor the release by changing the crosslink density [12–15].

Biodegradable dextran-based microspheres are prepared in an all-aqueous environment by crosslinking dextran derivatized with hydroxyethyl methacrylate (dex-HEMA) droplets in an emulsion with poly(ethylene glycol) (PEG) [14–16]. Under physiological conditions, the carbonate esters linking the poly-HEMA to the dextran are hydrolyzed, which results in an increased mesh size in the hydrogel network. The encapsulated protein will be released when the mesh size exceeds its hydrodynamic diameter. In previous studies it was shown that the release of entrapped colloidal particles (proteins, liposomes) from dex-HEMA microspheres could be tailored from days to months by varying the degree of substitution (DS, the number of hydroxyl ethyl methacrylates per 100 glucose units) of dextran and the initial water content of the microspheres [14,17].

To optimize the protein release characteristics of these systems, a fundamental understanding of the degradation mechanism, the diffusion of proteins through the matrix, as well as formulation parameters controlling the initial burst, the release rate, the lag time and the release time is required. The development of an appropriate model can be very helpful in

* Corresponding author. OctoPlus Technologies, OctoPlus b.v., Zernikedreef 12, 2333 CL, Leiden, The Netherlands. Tel.: +31 71 5271736; fax: +31 71 5244043.
E-mail address: wensink@octoplus.nl (K.D.F. Vlugt-Wensink).

0168-3659/$ - see front matter © 2005 Elsevier B.V. All rights reserved.
doi:10.1016/j.jconrel.2005.11.021

List of symbols

N_{model}	model parameter describing the maximum number of crosslinks per lattice site. In all simulations reported here, $N_{model}=2000$ (see Section 2.1)
X_{model}	model crosslink density; number of neighboring crosslinks that needs to be broken to open a lattice site. Note that X_{model} depends on two experimental parameters: the actual degree of substitution of dextran and the hydrodynamic diameter (d_h) of the protein.
D_{model}	rate at which a molecule jumps to a neighboring *open* lattice site
r	reaction rate
k	reaction rate constant: also hydrolysis rate constant
K	number of events
u	uniformly distributed random number between 0 and 1
M	number of cycles
$P(t)$	probability that a lattice site is open at time t
$\theta(t)$	Heaviside step function
P	protein loading
d_h	hydrodynamic diameter

the understanding and optimization of the release curves of these systems. Moreover, as experiments can be time and labor consuming, computer simulations may provide an attractive alternative to deepen the understanding of the release process.

In dex-HEMA based systems, the protein is surrounded by crosslinked dextran. For this system, protein release is controlled by the opening of domains inside the microsphere as a result of hydrolysis of crosslinks. Many models have been developed to describe the release of drugs from various drug delivery systems [18–24]. Most related to dextran-based microspheres are the PLA-*b*-PEG-*b*-PLA gels developed by West and Hubbell [25]. For these systems, Mason et al. [26] developed scaling laws that relate bulk-degradation to the changing transport properties of proteins during degradation. The predicted release curves agreed qualitatively with experimental observations. However, quantitative predictions were not possible, suggesting that not all important chemical and physical processes were taken into account properly.

Models describing the network changes at a microscopic level may result in better quantitative agreement between the model and experiments. Most models describing polymer degradation and release of proteins at microscopic level are based on Monte Carlo simulations [27–31]. An important advantage of this type of simulations is the use of a stochastic description of the state of a small domain inside the microsphere. Moreover, the effects of diffusion and degradation can be studied separately.

Important progress was made in the understanding of the degradation and release from bioerodible systems with models based on Monte Carlo simulations. Following the pioneering work of Zygourakis [27,28], Göpferich [29–31] and co-worker constructed a model in which the erosion of polymer 'pixels' (i.e. small domains inside a microsphere) was considered as a random event. This erosion was combined with the diffusion of degradation products. Good agreement was obtained between this model and available experimental data. To investigate the drug release from bioerodible spherical particles, a new mathematical model was developed by Siepmann et al. [32], in which a stochastic process described local erosion. Release curves were obtained by solving Fick's second law numerically with a diffusivity related to local erosion. At present, no microscopic models are available describing the release of proteins by hydrolysis of crosslinks and diffusion of proteins in matrices based on dextran, PLA-*b*-PEG-*b*-PLA and other related systems [25].

The aim of this study is to describe the release of proteins of variable size from dex-HEMA microspheres with different crosslink densities. For that purpose, a numerical model based on Monte Carlo simulations was developed which accurately describes the diffusion and degradation processes inside the microspheres, while neglecting swelling effects of the microspheres. After validation of the model with experimental release data of bovine serum albumin (BSA) monomer from dex-HEMA microspheres, scaling laws for the model diffusivity and model crosslink density with the hydrodynamic diameter of the protein were obtained. This was used to predict release curves for different crosslink densities and encapsulated proteins (hGH, IgG) and liposomes, for which experimental release curves were taken from earlier work of our group [14,17,33]. The experimental observations and the computed release curves combined with confocal microscopy experiments were used to obtain a better understanding of the processes determining the release from dex-HEMA based microspheres.

2. Theory

2.1. Hydrolysis of crosslinks and opening of lattice sites

In the experimental situation, prior to polymerization, the protein molecules are dissolved in a dex-HEMA solution. After polymerization, these molecules are entrapped inside the network if the initial mesh size of the network is smaller than their hydrodynamic diameter (Fig. 1).

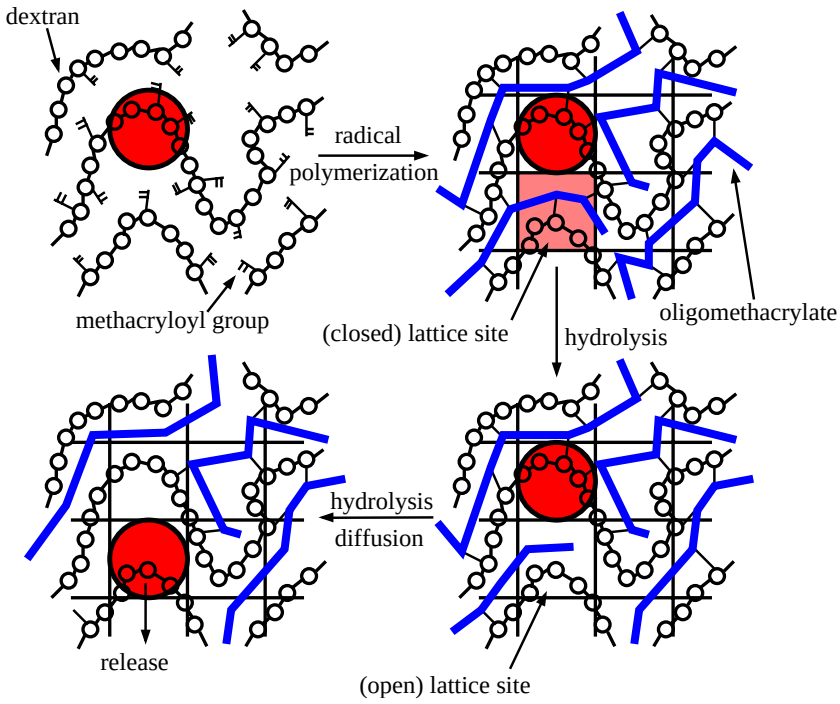

Fig. 1. Schematic two-dimensional representation of the confinement of a protein molecule and its subsequent release from dex-HEMA microspheres. Key features of the release are the opening of a neighboring lattice site through hydrolysis of crosslinks and the subsequent diffusion of a protein molecule to this lattice site.

The microsphere is modeled as a cubic three-dimensional lattice. For simplicity reasons, the lattice is modeled as a cubic object instead of a spherical object, as diffusion inside a spherical object and a cubic one only differ by a constant geometric factor. Each lattice site represents a small domain of the microsphere containing a certain number of crosslinks (Fig. 1). At time $t=0$ protein molecules are randomly distributed over the lattice sites. Two proteins can never occupy the same lattice site (excluded volume principle). No proteins are present at the surface lattice sites. Furthermore, when a protein molecule occupies a certain lattice site, no crosslinks are present at that site.

In the experiments, once a protein is entrapped inside the network (Fig. 1) the protein can only be released when (1) holes in the network are created through hydrolysis of the surrounding crosslinks, or, (2) swelling of the system creates a larger mesh size. Generally, swelling can occur directly after preparation (equilibrium swelling) and as a result of hydrolysis of crosslinks. It has been demonstrated before that after preparation, dex-HEMA microspheres immediately reach their equilibrium swelling [34]. It is expected that the swelling as a result of hydrolysis of crosslinks is not contributing to the opening of lattice sites, as the remaining crosslinks will keep the proteins entrapped in the network. Therefore, swelling is neglected in this model.

In principle, the opening of a small domain inside the microsphere is determined by microscopic parameters such as the average distance between two crosslinks, the size and shape of the protein, and the topology of the crosslinked network. This information can be used to construct a geometric model based on the caging of a certain object [35,36]. However, the precise details of the microscopic parameters controlling this confinement are unknown. Therefore, in this model, a coarse-grained approach was used to model the opening of a small domain inside the microsphere (represented by a lattice site). In this approach, a single lattice site is modeled as N_{model} crosslinks arranged on a line (Fig. 2A). The lattice site is considered open when at least X_{model} neighboring crosslinks are hydrolyzed. Periodic boundaries are applied to identify neighboring crosslinks near the edges.

The opening of lattice sites around a protein by hydrolysis of crosslinks is related to two experimental parameters: (1) the experimental crosslink density and (2) the hydrodynamic diameter (d_{h}) of the protein. The actual crosslink density is determined by the degree of HEMA substitution (DS) of dextran and the water content of the microspheres. For larger proteins or higher crosslink densities, more crosslinks need to be hydrolyzed to open a lattice site. This means that when N_{model} is fixed, X_{model} increases with protein size and crosslink density of the gel. It is important to note that different combinations of the protein size and actual crosslink density can in principle result in similar release curves. This implies that the experimental situation can be described by a model crosslink density X_{model} which depends on both the hydrodynamic diameter and the degree of HEMA substitution (DS), while keeping the maximum number of modeled crosslinks (N_{model}) fixed. Keeping N_{model} fixed for all simulations is allowed, as variations in the actual crosslink density (which in turn at fixed water content is proportional to the degree of HEMA substitution) or hydrodynamic diameter (d_{h}) are already accounted for in X_{model}. In that situation, it is assumed that X_{model} is directly proportional to the actual crosslink density (DS). The precise interplay between X_{model} and d_{h} will be discussed in Section 4.3.

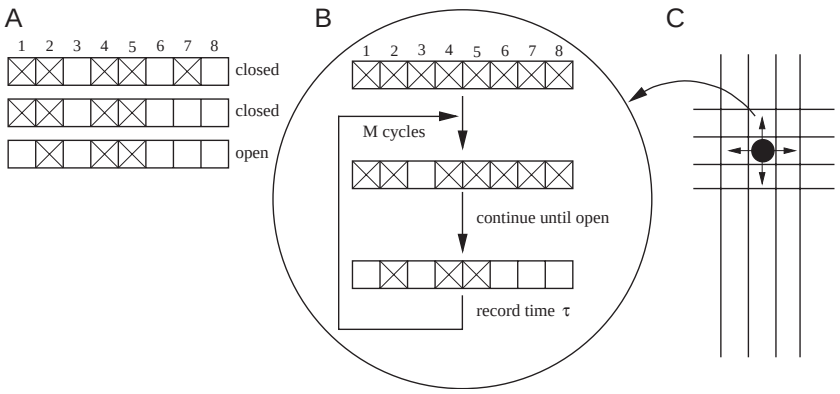

Fig. 2. Schematic representation of the model used in the simulations. (A) Example for the opening of a single lattice site with $N_{model}=8$ and $X_{model}=4$. The lattice site is considered open if four neighboring crosslinks are hydrolyzed. Periodic boundary conditions are applied. Intact crosslinks are indicated with a cross; hydrolyzed crosslinks are indicated with empty squares. (B) Schematic representation of the kinetic Monte Carlo scheme to compute $P(t)$ for a single lattice site, see also Eq. (3). ($N_{model}=8$, $X_{model}=4$). (C) Diffusion of a protein in the degrading matrix. A protein can jump to a neighboring lattice site (jump rate: D_{model}) provided that it is open. The time τ_i at which lattice site i is open is computed by solving $P(\tau_i)=u$, in which u is a uniformly distributed random number between 0 and 1. This is done for each lattice site at the start of the simulation.

Generally, the hydrolysis of crosslinks can be considered as independent events with rate constant k. Therefore, the degradation of the polymer network can be described by a Poisson process. The time evolution of a Poisson process can be followed by using the conventional kinetic Monte Carlo (KMC) scheme (see Section 3.1.1).

2.2. Protein diffusion inside a microsphere

At $t=0$ protein molecules are positioned at lattice sites. To model diffusion, it is assumed that a protein molecule can jump to a neighboring lattice site provided that it is "open", i.e. X_{model} crosslinks are hydrolyzed so that the protein can enter this new lattice site (see Section 2.1). Proteins jump to neighboring lattice sites with a certain rate: D_{model}. Attempted jumps to a "closed" lattice site are rejected, e.g. the protein returns to its original position. Proteins that leave the cubic three-dimensional lattice are considered as released. In this model it is assumed that jumps of protein molecules to neighboring lattice sites are uncorrelated. It is also assumed that hydrolysis of crosslinks and attempted jumps to neighboring lattice sites are uncorrelated processes as well. This means that it is possible to determine which lattice sites are open at time t before the start of the simulation.

3. Materials and methods

3.1. Modeling section

The modeling of the release of proteins from dex-HEMA based microspheres is split into two parts. The first part consists of modeling the hydrolysis of crosslinks and opening of lattice sites. This will provide a release curve for the opening of a single lattice site. This curve is used in the second part of the model, which describes the diffusion of proteins in the degrading polymer matrix and their subsequent release.

3.1.1. Hydrolysis of crosslinks and opening of lattice sites

Assuming that the average size of a microsphere is 10 μm and protein size is 10 nm (e.g. IgG, Table 1), a minimum

Table 1
Overview of parameters used in experiments and simulations

Protein	Experiments				Simulations		
	d_h [a] (nm)	DS	pH	Hydrolysis rate constant [b] (s^{-1})	P (% v/v)	D_{model}	X_{model}
BSA							
–Monomer (Mw=67 kDa)	7.2	12	7.2	$3.24\cdot10^{-6}$	7.9%	$1.0\cdot10^{-3}$	15
–Dimer	13.6	12				$5.3\cdot10^{-4}$	43
IgG [14] (Mw=150 kDa)	10.9	3	7.0	$2.06\cdot10^{-6}$	5.9%	$6.6\cdot10^{-4}$	9
		6					15
		8					20
		12					29
hGH [33] (Mw=22 kDa)	4.1	16	7.4	$5.09\cdot10^{-6}$	5.1%	$1.8\cdot10^{-3}$	8
Liposomes [6]	180	8	7.2	$3.24\cdot10^{-6}$	10% [c]	$4.0\cdot10^{-5}$	2000

[a] For IgG and BSA monomer d_h was taken from Ref. [17]. For hGH and BSA dimer d_h was derived using GPC data of Ref. [33].
[b] The rate constants were derived from the pH dependence of the hydrolysis rate constant k as previously reported by van Dijk-Wolthuis et al. [39].
[c] The loading of microspheres with liposomes was not given in Ref. [17]. Arbitrarily, a loading of 10% was assumed. In principle, any loading is justified since at low diffusivity the loading does not affect the release curve.

lattice size of $1000\times1000\times1000$ would be necessary to model each crosslink as a single lattice site. Simulations for these lattice dimensions are extremely time consuming. Therefore, the simulations were performed for a $50\times50\times50$ lattice in which each lattice site represents either a protein or a certain number of crosslinks. Lower lattice dimensions will result in insufficient resolution. Simulations of slightly larger lattice dimensions do not change our results significantly. Therefore, the use of a $50\times50\times50$ lattice is a compromise between resolution (large lattices) and computational resources (small lattices).

Each lattice site represents a certain number of crosslinks (here: $N_{\text{model}}=2000$), which is fixed as discussed in Section 2.1. To open a lattice site, X_{model} out of N_{model} crosslinks have to be hydrolyzed, see Fig. 2. The value of $N_{\text{model}}=2000$ is chosen in such a way that (1) the simulations are able to describe a wide range of protein sizes and DS's, and (2) for the largest particle in this study, $X_{\text{model}}=N_{\text{model}}$.

In this paragraph, the kinetic Monte Carlo scheme is described (see also Fig. 2B). In general, in the KMC algorithm the following steps are executed:

1. Set the time τ at $\tau=0$.
2. Construct a list of possible events (i.e. list of crosslinks that can be hydrolyzed). Suppose that there are K events with rate constants r_1, r_2, r_3,..r_K (in units of events per unit of time).
3. Select one of these events (l) with a probability
$$p_l = \frac{r_l}{\sum_{j=1}^{K} r_j} \tag{1}$$
4. Execute this particular event and advance the time for the next event ($i+1$) by
$$\tau_{i+1} = \tau_i + \frac{|\ln(u)|}{\sum_{j=1}^{K} r_j} \tag{2}$$
in which u is a uniformly distributed random number between 0 and 1.
5. Check whether X_{model} neighboring crosslinks are broken in such a way that the lattice site is open (Fig. 2A). If this is the case, record the time τ, otherwise return to step 2.
6. Repeat this process M times. Reasonable statistics were obtained with $M=10^6$.
7. Construct the cumulative distribution of τ by computing
$$P(t) = \frac{\sum_{i=1}^{M} \theta(t-\tau_i)}{M} \tag{3}$$
in which $\theta(t)$ is the usual Heaviside step function ($\theta(t)=1$ for $t>0$ and $\theta(t)=0$ otherwise). Essentially, $P(t)$ is the probability that X_{model} neighboring crosslinks out of N_{model} are hydrolyzed at time t. As τ can be written as a sum of exponentially distributed random variables, it is expected that the time derivative of $P(t)$ is Gaussian [37,38].

3.1.2. Protein diffusion inside a microsphere

At $t=0$, P protein molecules are distributed randomly over the lattice. Each lattice site can be either open or closed at a certain time t with a probability given by Eq. (3). A lattice site occupied with a protein molecule does not contain crosslinks. The time τ_i at which lattice site i is opened can be calculated by solving $P(\tau_i)=u$, in which u is a uniformly distributed random number between 0 and 1. This equation was solved for each lattice site at the beginning of the simulation. The function $P(t)$ is uniquely determined by X_{model} and N_{model} and was computed using the method outlined in the previous section.

After the start of the simulation, protein molecules (or other entrapped colloidal particles such as liposomes) can diffuse from lattice site to lattice site with diffusivity D_{model} (here defined as a jump rate, in units of particle jumps per unit of time) using the same KMC scheme as described in the previous section. Jumps to new lattice sites are accepted when the new lattice site is open and not occupied by another protein molecule, see Fig. 2C. Proteins that diffuse out of the lattice are marked as released. The simulation stops when all proteins have been released from the cubic lattice. The approximate CPU time for a typical simulation of protein release takes less than 5 min. Clusters of proteins were modeled as a group of monomeric proteins, in which each protein occupies a lattice site. For example, a cluster of $10\times10\times10$ proteins means a group of 1000 protein molecules occupying 1000 neighboring lattice sites. Once sufficient crosslinks are hydrolyzed, the protein molecules can move independently from each other to other open lattice sites. A cluster is not an aggregate, as the proteins are neither physically, nor chemically linked.

3.1.3. Comparison with in vitro release experiments

To compare the computed release curves with previously reported experimental release curves of BSA (see Section 3.2), IgG [14], hGH [33] and liposomes [17], the time in the simulations was converted to days using the hydrolysis rate constant k of dex-HEMA in solution (Table 1). The release curves for BSA monomer, BSA dimer, hGH and the liposomes were normalized (maximum release was set at 1). This was not possible for the curves of IgG as complete release was not obtained, and therefore the release curves were used as reported in Ref. [14].

For the simulations, the protein loading of the microspheres, in the experiments given in weight of protein/weight of dex-HEMA, was converted into protein volume/microsphere volume using an average microsphere size of 10 μm, a water content of 50%, the density of dextran (1.61 g/cm^3) [40] and the hydrodynamic diameters (d_h) and the molecular weights of the proteins (Table 1). The loading of microspheres with liposomes was arbitrarily set at 10% (volume of liposomes/volume of microsphere).

The relation between d_h and X_{model} and D_{model}, respectively, was determined in the following way. Initially, the experimental release curves of BSA monomer were fitted to the computed release curves to obtain the model crosslink density (X_{model}) and the model diffusivity (D_{model}) for BSA monomer. The experimental release curves of BSA dimer and liposomes were used to investigate the scaling of X_{model} and D_{model} with the

hydrodynamic diameter (d_h) of the protein. Using these scaling relations, X_{model} and D_{model} were calculated for IgG, hGH and liposomes (see Table 1) and their release curves were computed. Confocal microscopy analysis of fluorescently labelled protein in some systems indicated the presence of protein clusters. The size of these clusters is of the order of the size of a microsphere. For these systems, the release curves were computed assuming that the proteins were initially arranged in clusters of similar size ($10\times10\times10$ compared to $50\times50\times50$ for the whole lattice).

3.2. Experimental section

3.2.1. Materials

Poly(ethylene glycol) (PEG) 10,000 g/mol and potassium peroxodisulfate (KPS) were obtained from Merck (Darmstadt, Germany). *N,N,N′,N′*-tetramethyl ethylene diamine (TEMED), fluorescein isothiocyanate-bovine serum albumin (FITC-BSA) were purchased from Fluka (Buchs, Switzerland). Rhodamine B isothiocyanate was obtained from Aldrich (Milwaukee, USA). Bovine immunoglobulin G (IgG, fraction II) was purchased from ICN Biomedicals (Zoetermeer, The Netherlands). Hydroxyethyl methacrylate derivatized dextrans (dex-HEMA) with a degree of HEMA substitution 8 (8 HEMA groups per 100 glucose units) were synthesized according to van Dijk-Wolthuis et al. [41] and obtained from Polymer Service Centre Groningen (PSCG, Groningen, The Netherlands).

3.2.2. Preparation of rhodamine labeled IgG

A solution of 50 mg/ml IgG in phosphate buffer (10 mM) was incubated with rhodamine (ratio 1 : 5 mol/mol) for 1 day at room temperature under stirring. The IgG was separated from the rhodamine by diafiltration over 10 kDa filters.

3.2.3. Preparation of microspheres

Dextran microspheres were prepared by a water-in-water emulsion technique [16]. First, a dex-HEMA solution containing protein was prepared. This solution was obtained by dissolving 61 mg dex-HEMA in 488 mg buffer and 61 μl of a solution of 50 mg/ml rhodamine labeled IgG or in 427 mg buffer and 120 μl of a solution of 50 mg/ml FITC-labeled BSA or BSA. Second, 610 mg of dex-HEMA/protein solution was added to a PEG solution (3.75 g, 35% w/w). All solutions were prepared in 10 mM phosphate buffered saline pH 7.0. An emulsion was obtained by vortexing this mixture in a 15 ml tube (1 min, 14,000 min^{-1}). Then, 100 μl TEMED solution (20% v/v, pH neutralized with 4 M hydrochloric acid) was added. The emulsion was vortexed for another minute, and 180 μl of 50 mg/ml KPS-solution was added and polymerization was allowed to proceed for 60 min at room temperature, without stirring. Multiple centrifugation and washing steps were performed to purify the crosslinked dextran particles.

3.2.4. Confocal laser scanning microscopy

The microspheres were mixed with FluorSave (Calbiochem, San Diego, CA, USA) before visualization. Confocal microscopy analysis was performed with a Leica TCS-SP confocal laser scanning microscope equipped with a 488 nm Argon laser used to detect FITC-labeled BSA, 568 nm Krypton laser used to detect rhodamine labeled IgG. Laser power and photomultiplier settings were kept identical for all the samples.

3.2.5. In vitro release of BSA

The BSA loaded microspheres were resuspended in 5 ml 25 mM phosphate buffer pH = 7.0. Periodically, the microspheres were centrifuged for 7 min at 3200 ×*g*, 3 ml supernatant was removed and replaced by 3 ml 25 mM phosphate buffer pH = 7.4. The BSA monomer and dimer concentration was determined using size exclusion chromatography (SEC) [42].

4. Results and discussion

4.1. Hydrolysis of crosslinks and opening of lattice sites

In Fig. 3 the distributions $P(t)$ for different X_{model} (model crosslink density; number of neighboring crosslinks that need to be broken to open a lattice site) are plotted. As expected, as X_{model} increases, it will take on average more time to open a lattice site. All curves have an S-shape. The time derivative of $P(t)$ is the probability distribution of the release time τ. The release time τ was nearly Gaussian distributed in this model. This is as expected, since τ equals the sum of exponentially distributed random variables (Erlang distribution).

4.2. Modeling release

4.2.1. Diffusion

The effect of diffusivity on the computed release curves was investigated. Fig. 4 shows the computed cumulative release curves for a variable D_{model}, at a fixed protein loading of 10% and model crosslink density $X_{model} = 10$. For the whole range of tested model diffusivities, a biphasic release curve was observed. During the first phase, no protein was released. The duration of this phase, which is called the lag time, was almost

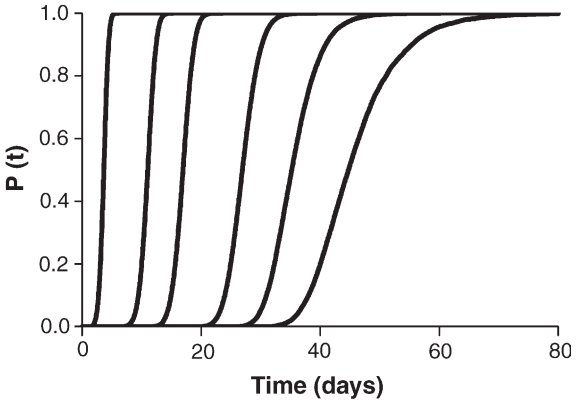

Fig. 3. Probability $P(t)$ that a lattice site is open at time t for $N_{model} = 2000$ and different model crosslink densities (X_{model}) as a function of time. Curves from left to right are for $X_{model} = 10$, 40, 100, 400, 1100 and 2000. To convert the time in units of $1/k$ to time in days, a hydrolysis rate constant of $2.06\cdot10^{-6}$ s^{-1} was used (Table 1).

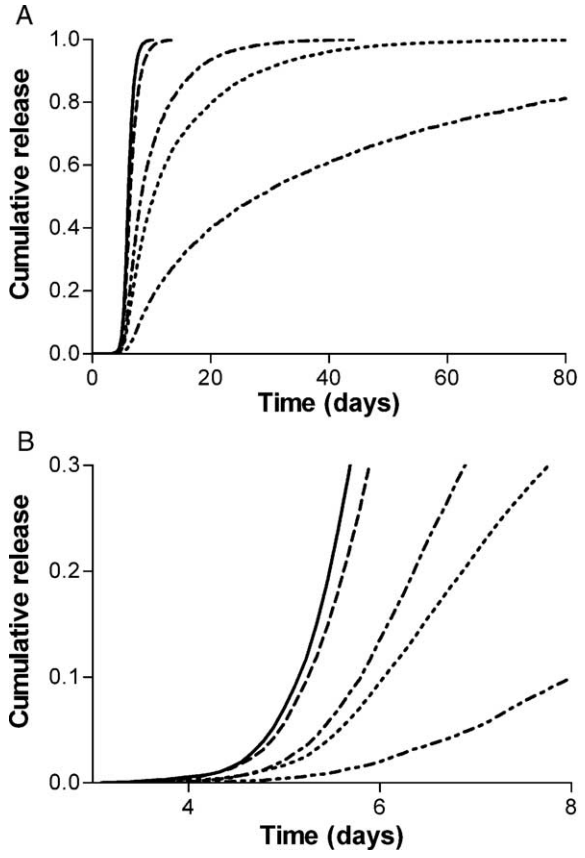

Fig. 4. (A) Computed release curves of proteins from microspheres as function of time for a range of D_{model}. From left to right: $D_{model}=5\cdot10^{-1}$; $1\cdot10^{-1}$; $1\cdot10^{-2}$; $1\cdot10^{-3}$; $1\cdot10^{-4}$ (Note: loading=10%, $X_{model}=10$, protein molecules are homogeneously distributed over the lattice, hydrolysis rate constant=$2.06\cdot10^{-6}$ s^{-1}). (B) Release during the first 8 days.

independent of diffusivity (see Fig. 4B, lag time is around 4 days). In the second phase, the protein was released with a diffusion dependent release rate. During the first phase, crosslinks are hydrolyzed and some lattice sites are opened. However, not enough neighboring lattice sites are opened to release the protein from the matrix. In the second phase, when sufficient neighboring lattice sites are opened, protein molecules can jump from one lattice site to another and can consequently be released from the matrix. Fig. 4 also clearly shows that the release kinetics after the lag time strongly depended on D_{model}. When D_{model} is increased from 10^{-4} to 10^{-2}, the release rate increases and the total release time (time to release all protein molecules) decreases. Assuming that the diffusivity of a protein is related to its size (Stokes–Einstein equation), for large proteins diffusion becomes the rate determining process, resulting in a substantially decreased release rate and also longer total release time. Note that for larger proteins the lag time will also increase because X_{model} increases.

4.2.2. Model crosslink density, protein loading and clusters

The effect of X_{model} on the release of proteins with different sizes, and thus different D_{model}, from the microspheres is shown in Fig. 5. In these simulations, again biphasic release curves were found. In this figure it is shown that the lag time of the first phase depends on X_{model} (~4 and 7 days for $X_{model}=16$ and 30, respectively). The release rate in the second phase was nearly independent of X_{model}, but strongly dependent on D_{model} (see also Fig. 4).

The effect of protein loading is also shown in Fig. 5. At higher protein loading the lag time is slightly shorter (~0.5 day shorter, comparing protein loading=4% and 25% at $X_{model}=30$, $D_{model}=1\cdot10^{-2}$). If the protein molecules are initially homogeneously distributed over the lattice, more protein molecules are present close to the surface of the microspheres at higher protein loading. Since less lattice sites need to be opened to release proteins close to the surface, the release from microspheres with a higher loading starts consequently earlier. This effect becomes less pronounced at smaller D_{model} (larger proteins).

Tuinier and Brulet [43] showed that phase separation of lysozyme in a dextran solution occurred at low dextran concentrations (<15% w/w) and low lysozyme concentrations. Likely, phase separation will also occur for other proteins in the highly concentrated dex-HEMA phase (50% w/w). As a result, after polymerization, clusters of protein are imprisoned in the network of the microspheres. With the currently developed model, the effect of clusters of proteins on the release curves was investigated. At low loading (4% v/v) and small X_{model} the effect of the clusters on the release curves was marginal. After the lag time (which was almost independent of the presence of clusters) the release rate is slightly higher for proteins homogeneously distributed over the microspheres than for proteins originally present in clusters (data not shown). This can be explained by the restricted mobility of proteins inside a cluster. Before proteins inside a cluster are able to move, first proteins at a neighboring lattice sites should have jumped at other (unoccupied) lattice sites. Only for large X_{model} and at high loading the effect of clusters becomes important. At $X_{model}=30$, $D_{model}=10^{-3}$ and loading=25% v/v, the release curve of proteins from microspheres with clusters was shifted and the time to release 50% of the entrapped protein was increased from 8 to 9.5 days. It is important to note that of the effect of X_{model} on the release is much larger than the effects of loading and clusters.

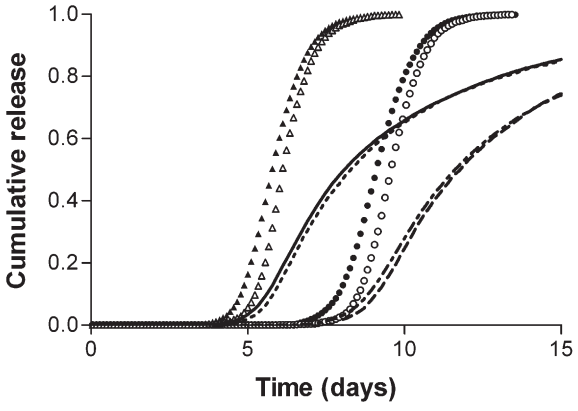

Fig. 5. Computed release curves of proteins from microspheres as function of time. $X_{model}=16$ (▲, Δ or - - -,—), 30 (●, ○ or – - –,– –), loading 25% (closed symbols, — or – – –) and 4% (open symbols, - - - or — —), $D_{model}=1\cdot10^{-2}$ (symbols) and $1\cdot10^{-3}$ (lines) (hydrolysis rate constant=$2.06\cdot10^{-6}$ s^{-1}).

4.3. Validation and prediction

As no length scales were introduced for the lattice or a single lattice site, the model crosslink density (X_{model}) and the model diffusivity (D_{model}) cannot be converted directly into experimental diffusion and crosslink densities. Therefore, to compare the experimental release curves with the simulations, the experimental crosslink density should be translated into the model crosslink density (X_{model}). Moreover, a D_{model} should be fitted, representing the diffusion of proteins inside a microsphere. The release of BSA monomer obtained from dex-HEMA microspheres (DS 12) was fitted with the computed release curves. Fig. 6A shows a confocal microscopy image of microspheres loaded with FITC-BSA. This suggests that BSA is homogeneously distributed over the microspheres and in the simulations it was therefore assumed that the BSA molecules were homogeneously distributed over the lattice. The best fit was obtained using $X_{model}=15$ and $D_{model}=1.0\cdot10^{-3}$ (Fig. 7). The simulation is in good agreement with experimental data.

The obtained X_{model} and D_{model} for BSA monomer (Table 1), and the experimental release curves of BSA dimer and liposomes were used to investigate the scaling of X_{model} and D_{model} with the hydrodynamic diameter (d_h). To compute the release curve of liposomes from the microspheres, it was assumed that D_{model} is proportional to $1/d_h$ (Stokes–Einstein equation), in which d_h is

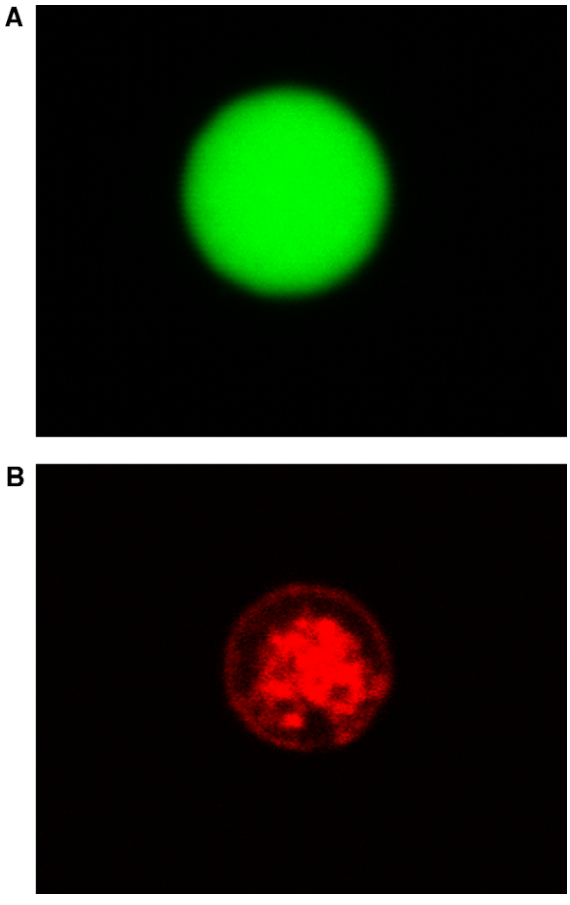

Fig. 6. (A) FITC-BSA and (B) rhodamine labeled IgG encapsulated in dex-HEMA microspheres (DS 12, water content 50%).

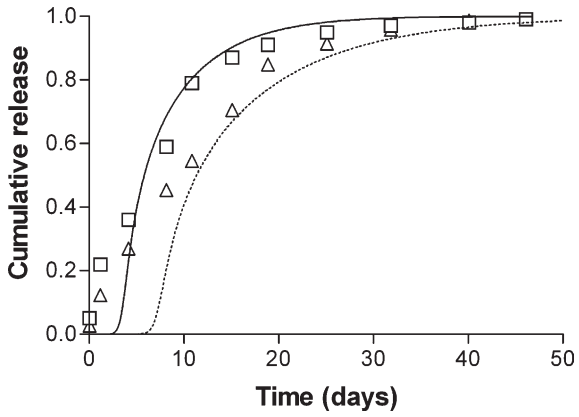

Fig. 7. Cumulative release of BSA monomer (□) and dimer (Δ) from dex-HEMA microspheres (DS 12, water content of 50%) as a function of time. The computed release curves are plotted as lines.

the hydrodynamic diameter of the liposome. Furthermore, with increasing protein (or liposome) size X_{model} increases since for a larger protein (or liposome) more crosslinks need to be hydrolyzed to open a lattice site. However, the precise relation between X_{model} and d_h is not a priori clear. There are two extreme situations that result in opening of the lattice site and release of the protein (or liposome) (Fig. 8). In the first situation, a lattice site is opened when all crosslinks at the perimeter of the projection of the protein on the plane are hydrolyzed. This means that X_{model} is proportional to d_h. In the second situation, a lattice site is open when all crosslinks at the surface of the projection of the protein are hydrolyzed. In that particular case, X_{model} scales with d_h^2. The real situation is expected to be an intermediate between these two extreme situations, as crosslinks are hydrolyzed randomly and not exclusively on the perimeter of the projected protein. Moreover, not all crosslinks on the projected area of the protein need to be hydrolyzed to open a lattice site. Therefore, it is expected that X_{model} scales with d_h^{α}, where $1<\alpha<2$.

In Fig. 9, the experimental and computed release curves of liposomes from dex-HEMA microspheres are shown. Best agreement between experimental data and simulations was obtained by

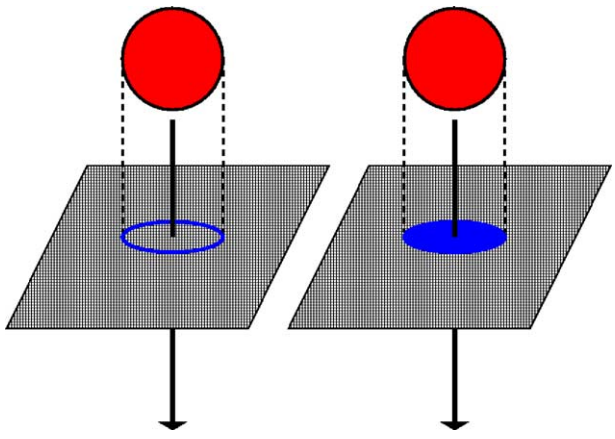

Fig. 8. Schematic representation of the movement of a protein through a plane of crosslinks. There are two extreme situations. Left: Crosslinks are hydrolyzed at the perimeter of the projection of the protein onto the plane. Right: Crosslinks at the projection of the protein are hydrolyzed.

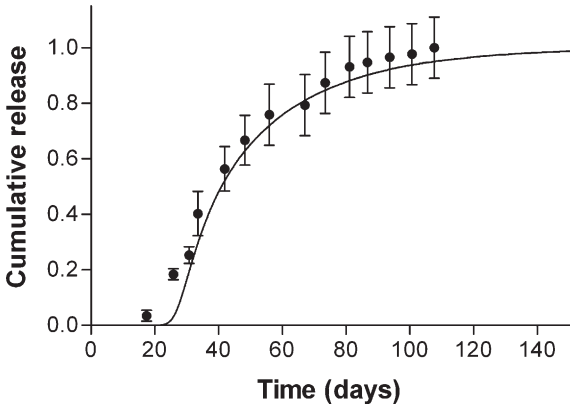

Fig. 9. Cumulative release of liposomes from dex-HEMA microspheres (DS 8 (●), water content 50%) as a function of time obtained previously by Stenekes et al. [17]. The computed release curve is plotted as a solid line.

using $X_{model}=2000$ and $D_{model}=2.0\cdot10^{-5}$ and $\alpha=1.64$. Note that for liposomes X_{model} equals N_{model}, which means that liposomes can only jump to neighboring lattice sites when all model crosslinks are hydrolyzed (Fig. 2A). The Stokes–Einstein relation predicts a somewhat higher diffusivity ($D_{model}=4.0\cdot10^{-5}$, Table 1). This may indicate that in the degrading hydrogel matrix the mobility of liposomes is more restricted than that of BSA.

Based on the values for X_{model} and D_{model} obtained for BSA monomer as well as α (obtained from the release of the liposomes), X_{model} and D_{model} were calculated for BSA dimer, IgG and hGH released from dex-HEMA based microspheres using the scaling rules for crosslink density ($X_{model}\sim d_h^{1.64}$) and diffusivity ($D_{model}\sim 1/d_h$) as discussed in the previous paragraph. In Figs. 7, 10 and 11 the experimental data are compared with the simulations.

By applying the scaling relations, for BSA dimer $X_{model}=43$ and $D_{model}=5.3\cdot10^{-4}$ was predicted. Good agreement between experimental and computed release curve was obtained particularly for the last period of the release curve. Fig. 10 shows the computed and experimental release curves for IgG loaded microspheres. Confocal microscopy revealed that IgG is present

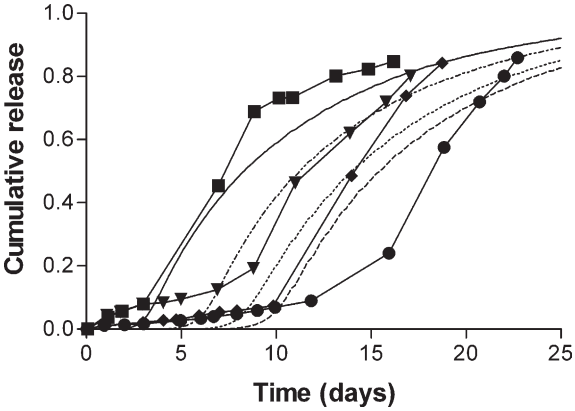

Fig. 10. Cumulative release of IgG from microspheres of DS 3 (■), DS 6 (▲), DS 8 (●) and DS 11 (♦) (water content 50%) as a function of time. Experimental data were obtained previously by Franssen et al. [14]. The computed release curves are plotted as lines. It was assumed that the proteins were present in clusters occupying 1000 lattice sites.

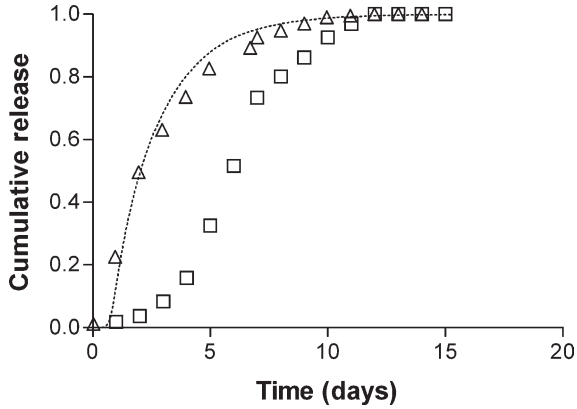

Fig. 11. Cumulative release of hGH as a function of time from microspheres of DS 16 and water content 50% prepared in the absence (□), and presence (Δ) of 0.1% tween 80. Experimental data were obtained by Vlugt-Wensink et al. [33]. The computed release curve is plotted as a line. In these simulations proteins were present in clusters occupying 1000 lattice sites.

in clusters of proteins inside the microsphere (Fig. 6B). Therefore, in the simulations of these systems the proteins were initially arranged in clusters. Good agreement was obtained between experimental and computed release curves, especially for the release of IgG from microspheres of DS 3 and 6 ($X_{model}=9$ and 15, respectively, $D_{model}=6.6\cdot10^{-4}$). Differences in the lag time (but not in release rate) between experiments and simulations were found for DS 8 and DS 11($X_{model}=20$ and 29, respectively, $D_{model}=6.6\cdot10^{-4}$) indicating that other processes than degradation and diffusion affect the release here. A possible explanation is that IgG is present as precipitates in the microspheres. A longer lag time can be expected when dissolution of IgG from the precipitates is rate-limiting.

Fig. 11 shows the experimental release curves for hGH from micropheres prepared in the presence and absence of 0.1% tween 80. In the release curve of hGH a lag time of 2 days is observed, where in the release curve of hGH with tween 80 no lag time was present. Moreover, the release rate of the hGH is quite similar. Good agreement was found between the experimentally obtained release curve of hGH from micropheres prepared with 0.1% tween 80 and the computed release curve ($X_{model}=16$, $D_{model}=1.8\cdot10^{-3}$). A possible explanation is that hGH without tween 80 is aggregated in the microspheres. Since aggregates are larger than monomers, a longer lag time and a lower diffusivity were expected. The difference in diffusivity for hGH monomer and dimer is relatively small and might not be observed in in vitro release experiments. In fact, experiments presented in Ref. [33] showed that when microspheres were prepared without tween, large precipates of hGH were observed. Therefore, the release of hGH does not only depend on hydrolysis and diffusion (processes included in this model), but probably also on the dissolution rate of these precipitates of hGH in these microspheres.

5. Conclusions

A model was developed to investigate the release of proteins from dex-HEMA based microspheres. The effects of

diffusion, crosslink density, protein loading, and clustering of proteins on the release were investigated. It was found that of the effect of X_{model} on the release is much larger than the effects of loading and clusters. It was shown that proper prediction of release curves is possible for various proteins and for microspheres of various crosslink densities (here: degree of substitution, DS) by scaling X_{model} with the hydrodynamic diameter $d_h^{1.64}$ and D_{model} with $1/d_h$ (Stokes–Einstein relation). As experimental determination of release kinetics can be time and labor consuming, this model may play an important role in the optimization, understanding and prediction of the release of various proteins from crosslinked hydrogel-based microspheres.

References

[1] P. van de Wetering, A.T. Metters, R.G. Schoenmakers, J.A. Hubbell, Poly (ethylene glycol) hydrogels formed by conjugate addition with controllable swelling, degradation, and release of pharmaceutically active proteins, J. Control. Release 102 (2005) 619–627.

[2] T. Kissel, Y. Li, F. Unger, ABA-triblock copolymers from biodegradable polyester A-blocks and hydrophilic poly(ethylene oxide) B-blocks as a candidate for in situ forming hydrogel delivery systems for proteins, Adv. Drug Deliv. Rev. 54 (2002) 99–134.

[3] K.S. Anseth, A.T. Metters, S.J. Bryant, P.J. Martens, J.H. Elisseeff, C.N. Bowman, In situ forming degradable networks and their application in tissue engineering and drug delivery, J. Control. Release 78 (2002) 199–209.

[4] J.M. Bezemer, D.W. Grijpma, P.J. Dijkstra, C.A. van Blitterswijk, J. Feijen, A controlled release system for proteins based on poly(ether ester) block-copolymers: polymer network characterization, J. Control. Release 62 (1999) 393–405.

[5] W.E. Hennink, O. Franssen, W.N.E. van Dijk-Wolthuis, H. Talsma, Dextran hydrogels for the controlled release of proteins, J. Control. Release 48 (1997) 107–114.

[6] N.A. Peppas, P. Buresa, W. Leobandunga, H. Ichikawa, Hydrogels in pharmaceutical formulations, Eur. J. Pharm. Biopharm. 50 (2000) 27–46.

[7] K. Kofuji, H. Akamine, H. Oshirabe, Y. Maeda, Y. Murata, S. Kawashima, Retention and release behavior of insulin in chitosan gel beads, J. Biomater. Sci., Polym. Ed. 14 (2003) 1243–1253.

[8] J.A. Cadée, C.J. de Groot, W. Jiskoot, W. den Otter, W.E. Hennink, Release of recombinant human interleukin-2 from dextran-based hydrogels, J. Control. Release 17 (2002) 1–13.

[9] J. Kuijpers, P.B. van Wachem, M.J.A. van Luyn, G.H.M. Engbers, J. Krijgsveld, S.A.J. Zaat, J. Dankert, J. Feijen, In vivo and in vitro release of lysozyme from cross-linked gelatin hydrogels: a model system for the delivery of antibacterial proteins from prosthetic heart valves, J. Control. Release 67 (2000) 323–336.

[10] J.A. Cadée, L.A. Brouwer, W. den Otter, W.E. Hennink, M.J. van Luyn, A comparative biocompatibility study of microspheres based on crosslinked dextran or poly(lactic-*co*-glycolic) acid after subcutaneous injection in rats, J. Biomed. Mater. Res. 56 (2001) 600–609.

[11] B.H. Woo, G. Jiang, Y.W. Jo, P.P. DeLuca, Preparation and characterization of a composite PLGA and poly(acryloyl hydroxyethyl starch) microsphere system for protein delivery, Pharm. Res. 18 (2001) 1600–1606.

[12] P. Martens, T. Holland, K.S. Anseth, Synthesis and characterization of degradable hydrogels formed from acrylate modified poly(vinyl alcohol) macromers, Polymer 43 (2002) 6093–6100.

[13] I.S. Kim, Y.I. Jeong, D.H. Kim, Y.H. Lee, S.H. Kim, Albumin release from biodegradable hydrogels composed of dextran and poly(ethylene glycol) macromer, Arch. Pharm. Res. 24 (2001) 69–73.

[14] O. Franssen, L. Vandervennet, P. Roders, W.E. Hennink, Chemically degrading dextran hydrogels: controlled release of a model protein from cylinders and microspheres, J. Control. Release 60 (1999) 211–221.

[15] W.N.E. van Dijk-Wolthuis, S.K.Y. Tsang, M.J. van Steenbergen, C. Hoogeboom, W.E. Hennink, Degradation and release behavior of dextran based hydrogels, Macromolecules 30 (1997) 4639–4645.

[16] R.J.H. Stenekes, O. Franssen, E.M.G. van Bommel, D.J.A. Crommelin, W. E. Hennink, The preparation of dextran microspheres in an all-aqueous system: effect of the formulation parameters on particle characteristics, Pharm. Res. 15 (1998) 557–561.

[17] R.J.H. Stenekes, A.E. Loebis, C.M. Fernandes, D.J.A. Crommelin, W.E. Hennink, Controlled release of liposomes from biodegradable dextran microspheres: a novel delivery concept, Pharm. Res. 17 (2000) 690–695.

[18] P. Martens, A.T. Metters, K.S. Anseth, C.N. Bowman, A generalized bulk-degradation model for hydrogel networks formed from multivinyl cross-linking molecules, J. Phys. Chem., B 105 (2001) 5131–5138.

[19] B. Amsden, A model for osmotic pressure driven release from cylindrical rubbery polymer matrices, J. Control. Release 93 (2003) 249–258.

[20] N.A. Peppas, Analysis of Fickian and non-Fickian drug release from polymers, Pharm. Acta Helv. 60 (1985) 110–111.

[21] L.K. Huang, R.C. Mehta, P.P. DeLuca, Evaluation of a statistical model for the formation of poly [acryloyl hydroxyethyl starch] microspheres, Pharm. Res. 14 (1997) 475–482.

[22] J.M. Bezemer, R. Radersma, D.W. Grijpma, P.J. Dijkstra, J. Feijen, C.A. van Blitterswijk, Zero-order release of lysozyme from poly(ethylene glycol)/poly(butylene terephthalate) matrices, J. Control. Release 64 (2000) 179–192.

[23] D.G. Kanjickal, S.T. Lopina, Modeling of drug release from polymeric delivery systems — a review, Crit. Rev. Ther. Drug Carr. Syst. 21 (2004) 345–386.

[24] J. Siepmann, A. Göpferich, Mathematical modeling of bioerodible, polymeric drug delivery systems, Adv. Drug Deliv. Rev. 48 (2001) 229–247.

[25] J.L. West, J.A. Hubbell, Photopolymerized hydrogel materials for drug delivery applications, React. Polym. 25 (1995) 139–147.

[26] M.N. Mason, A.T. Metters, C.N. Bowman, K.S. Anseth, Predicting controlled-release behavior of degradable PLA-*b*-PEG-*b*-PLA hydrogels, Macromolecules 34 (2001) 4630–4635.

[27] K. Zygourakis, Discrete simulations and bioerodible controlled release systems, Polym. Prep. ACS 30 (1989) 456–457.

[28] K. Zygourakis, Development and temporal evolution of erosion fronts in bioerodible controlled release devices, Chem. Eng. Sci. 45 (1990) 2359–2366.

[29] A. Göpferich, Mechanisms of polymer degradation and erosion, Biomaterials 17 (1996) 103–114.

[30] A. Göpferich, R. Langer, Modeling monomer release from bioerodible polymers, J. Control. Release 33 (1995) 55–69.

[31] A. Göpferich, Modeling of polymer erosion, Macromolecules 26 (1993) 4105–4112.

[32] J. Siepmann, N. Faisant, J.-P. Benoit, A new mathematical model quantifying drug release from bioerodible microparticles using Monte Carlo simulations, Pharm. Res. 19 (2002) 1885–1893.

[33] K.D.F. Vlugt-Wensink, Y.J. Meijer, R. Verrijk, W. Jiskoot, D.J.A. Crommelin, W.E. Hennink, Effect of excipients on the release of hGH from dex-HEMA microspheres, *Manuscript in preparation*.

[34] R.J.H. Stenekes, S.C. de Smedt, J. Demeester, G. Sun, Z. Zhang, W.E. Hennink, Pore sizes in hydrated dextran microspheres, Biomacromolecules 1 (2000) 696–703.

[35] A.P. Philipse, Caging effects in amorphous hard-spheres solids, Coll. Surf. A 213 (2003) 167–173.

[36] E.A.J.F. Peters, M. Kollmann, Th.M.A.O.M. Barenburg, A.P. Philipse, Caging of a d-dimensional sphere and its relevance for the random dense sphere packing, Phys. Rev., E 63 (2001) 021404.

[37] W. Feller, The fundamental limit theorems in probability, Bull. Am. Math. Soc. 51 (1945) 800–832.

[38] H.F. Trotter, An elementary proof of the central limit theorem, Arch. Math. 10 (1959) 226–234.

[39] W.N.E. van Dijk-Wolthuis, M.J. van Steenbergen, W.J.M. Underberg, W. E. Hennink, Degradation kinetics of methacrylated dextrans in aqueous solution, J. Pharm. Sci. 86 (1997) 413–417.

[40] N. Errington, S.E. Harding, L. Illum, E.H. Schacht, Physico-chemical studies on di-iodotyrosine dextran, Carbohydr. Polym. 18 (1992) 289–294.
[41] W.N.E. van Dijk-Wolthuis, S.K.Y. Tsang, J.J. Kettenes-van den Bosch, W. E. Hennink, A new class of polymerizable dextrans with hydrolyzable groups: hydroxyethyl methacrylated dextran with and without oligolactate spacer, Polymer 38 (1997) 6235–6242.
[42] M. van de Weert, M.J. Van Steenbergen, J.L. Cleland, J. Heller, W.E. Hennink, D.J.A. Crommelin, Semisolid, self-catalyzed poly(ortho ester)s as controlled-release systems: protein release and protein stability issues, J. Pharm. Sci. 91 (2002) 1065–1074.
[43] R. Tuinier, A. Brulet, On the long-range attraction between proteins due to nonadsorbing polysaccharide, Biomacromolecules 4 (2003) 28–31.